The American Journal of Pathology, Vol. 184, No. 5, May 2014

The American Journal of
PATHOLOGY
ajp.amjpathol.org

MOLECULAR PATHOGENESIS OF GENETIC AND INHERITED DISEASES

Bortezomib Partially Improves Laminin α2 Chain–Deficient Muscular Dystrophy

Zandra Körner,* Cibely C. Fontes-Oliveira,* Johan Holmberg,* Virginie Carmignac,† and Madeleine Durbeej*

From the Muscle Biology Unit, Department of Experimental Medical Science, Lund University, Lund, Sweden; and the Genetics of Developmental Abnormalities Team,† EA4271, University of Burgundy, Dijon, France*

Accepted for publication January 14, 2014.

Address correspondence to Madeleine Durbeej, Ph.D., Lund University, Muscle Biology Unit, Department of Experimental Medical Science, BMC B12, 221 84 Lund, Sweden. E-mail: madeleine.durbeej-hjalt@med.lu.se.

Congenital muscular dystrophy, caused by mutations in *LAMA2* (the gene encoding laminin α2 chain), is a severe and incapacitating disease for which no therapy is yet available. We have recently demonstrated that proteasome activity is increased in laminin α2 chain–deficient muscle and that treatment with the nonpharmaceutical proteasome inhibitor MG-132 reduces muscle pathology in laminin α2 chain–deficient dy^{3K}/dy^{3K} mice. Here, we explore the use of the selective and therapeutic proteasome inhibitor bortezomib (currently used for treatment of relapsed multiple myeloma and mantle cell lymphoma) in dy^{3K}/dy^{3K} mice and in congenital muscular dystrophy type 1A muscle cells. Outcome measures included quantitative muscle morphology, gene and miRNA expression analyses, proteasome activity, motor activity, and survival. Bortezomib improved several histological hallmarks of disease, partially normalized miRNA expression (miR-1 and miR-133a), and enhanced body weight, locomotion, and survival of dy^{3K}/dy^{3K} mice. In addition, bortezomib reduced proteasome activity in congenital muscular dystrophy type 1A myoblasts and myotubes. These findings provide evidence that the proteasome inhibitor bortezomib partially reduces laminin α2 chain–deficient muscular dystrophy. Investigation of the clinical efficacy of bortezomib administration in congenital muscular dystrophy type 1A clinical trials may be warranted. *(Am J Pathol 2014, 184: 1518–1528; http://dx.doi.org/10.1016/j.ajpath.2014.01.019)*

Congenital muscular dystrophy type 1A (MDC1A) is a severe form of muscular dystrophy for which there is currently no cure. Patients exhibit severe muscle hypotonia early in life, general muscle weakness accompanied by joint contractures, and few children achieve the ability to walk. Critical complications of MDC1A include respiratory failure and feeding problems, but noninvasive ventilation and gastrostomy can significantly improve health. Nonetheless, respiratory-tract infection is the most common cause of death, and approximately 30% of patients die within the first decade of life.[1,2] MDC1A is caused by mutations in the *LAMA2* gene; this gene encodes the laminin α2 subunit of the heterotrimeric protein laminin-211, which is a major constituent of basement membranes in the neuromuscular system. In MDC1A, laminin α2 chain expression is absent or significantly reduced, which leads to disrupted basement membranes and reduced cell interactions.[3–5] Laminin α2 chain binds two major cell surface receptors on muscle cells, namely, dystroglycan and integrin α7β1.[6–8] Thus, the structural link from the extracellular matrix to the cytoskeleton that stabilizes the muscle cell membrane and protects it from contraction-induced damage is disrupted in MDC1A.[9,10] Moreover, the expression of dystroglycan and in particular of integrin α7β1 is dysregulated in MDC1A,[11–13] and so downstream intracellular signaling pathways are also interrupted in MDC1A. Laminin α2 chain–deficient muscle fibers undergo degeneration–regeneration cycles, but eventually regeneration can no longer be maintained and consequently muscle

Supported by the Muscular Dystrophy Association (M.D.), the French Association against Myopathies (Association Française contre les Myopathies) (M.D.), the Crafoord Foundation (J.H.), the Kock Foundation (M.D.), the Alfred Österlund Foundation (M.D.), and the Swedish Research Council (M.D. and J.H.).

C.C.F.O. and J.H. contributed equally to this work.

Disclosures: V.C. and M.D. are cofounders and have equity ownership in the company MD Pharma AB, formed together with Lund University Bioscience AB. MD Pharma AB is the owner of intellectual property rights related to inhibition of autophagy and proteasome processes for treatment of muscular disorders.

http://dx.doi.org/10.1016/j.ajpath.2014.01.019

fibers die (enhanced apoptosis is a significant feature of MDC1A); this is followed by a major replacement of muscle tissue with connective tissue.[14–16]

There are several mouse models for MDC1A that, in general, accurately recapitulate the pathology of MDC1A.[16] Over the last decade, our research group has used the most severely affected dy^{3K}/dy^{3K} mouse, which is the only strain that completely lacks laminin α2 chain.[17,18] The median survival of dy^{3K}/dy^{3K} mice is approximately 22 to 23 days, and at time of death these mice exhibit severe muscle wasting.[17,19–22] Several approaches to combat disease in laminin α2 chain–deficient mouse models have been undertaken, and successful methods include transgenic overexpression of laminin α2 chain,[23] laminin α1 chain,[19] miniagrin,[12,24,25] integrin α7 subunit,[26] Bcl-2,[27] and IGF-1,[28] as well as pharmacological treatment with antiapoptotic[29,30] and antifibrotic[31,32] compounds or protein therapy with laminin-111.[33] Despite encouraging results to date, clinical applications are still years away.

Recently, our research group demonstrated that proteasome activity and autophagy are increased in laminin α2 chain–deficient muscle and that separate inhibition of each system significantly improves muscle morphology in a mouse model of MDC1A.[34,35] However, although these initial studies constitute proof-of-concept validation, neither of the inhibitors used (MG-132 and 3-methyladenine) is suitable for clinical testing. In the present study, therefore, we explored the use of the proteasome inhibitor bortezomib, which is used for treatment of relapsed multiple myeloma and mantle cell lymphoma.[36,37] We found that bortezomib has beneficial effects in laminin α2 chain–deficient dy^{3K}/dy^{3K} mice and in MDC1A patient cells.

Materials and Methods

Transgenic Animals

The laminin α2 chain–deficient dy^{3K}/dy^{3K} mice and dy^{3K}δE3 mice used have been described previously.[17,21,34] Dy^{2J}/dy^{2J} (B6.WK-Lama2$^{dy\text{-}2J}$/J), *mdx* (C57BL/10Scsn-mdx/J), β-sarcoglycan–deficient (B6.129-Sgcb^{tm1Kcam}/1J),[38] and integrin α7–deficient mice (B6.129-Itga7^{tm1Burk}/J) were obtained from the Jackson Laboratory (Bar Harbor, ME) and bred in our animal facility. The dy^{3K}/dy^{3K}, dy^{2J}/dy^{2J}, dy^{3K}δE3, and integrin α7–deficient mice were compared with wild-type (WT) littermates, and the *mdx* and β-sarcoglycan–deficient mice were compared with aged-matched WT mice (C57BL/6). Mice were maintained in the animal facilities of the Biomedical Center at Lund according to institutional animal care guidelines, and permission was given by the Malmö/Lund (Sweden) ethical committee for animal research (ethical permit numbers M15-12 and M279-12).

Bortezomib Treatment

Bortezomib was purchased from LC Laboratories (Woburn, MA). A stock solution dissolved in dimethyl sulfoxide was prepared, stored at −80°C, and then diluted in 100 μL sterile sodium chloride. The bortezomib (0.4 mg/kg) was injected into the tail vein of dy^{3K}/dy^{3K} and WT mice at 2.5 weeks of age and again at 3.5 weeks. Mice were sacrificed at 14 days after the second injection. Quadriceps and diaphragm muscles were processed for morphometric analysis or immunofluorescence experiments. Plasma analyses of cystatin-C were performed at the Clinical Laboratory at Skåne University Hospital (Lund, Sweden).

For cell cultures (described below), bortezomib was resuspended in dimethyl sulfoxide to obtain a 10 mmol/L solution. Dilutions of 1 and 10 nmol/L of bortezomib in growth medium for 24 hours were used for treatment of myoblasts. For myotubes, cell extracts were treated with 10 nmol/L of bortezomib for the 15 minutes before measurement of proteasome activity. No significant differences were observed between growth medium with dimethyl sulfoxide or left untreated; untreated growth medium was therefore used as control medium.

Cell Culture

Primary myoblasts (passage 2 to 3) were obtained from a control fetus (12 weeks of gestation) and from an MDC1A fetus (15 weeks of gestation) presenting a homozygous nonsense mutation in exon 31 of the *LAMA2* gene.[39] Muscle cells were obtained in accordance with French legislation on ethical rules for research involving humans. Cells were cultivated with F10–Ham's medium (Life Technologies, Carlsbad, CA) containing 20% fetal bovine serum (Life Technologies) at 37°C and 5% CO_2 in plastic flasks. To induce differentiation, cells were cultured in Dulbecco's modified Eagle's medium with GlutaMAX supplemented with 2% horse serum for 8 days. Plates were treated with Geltrex LDEV-free basement membrane matrix (Life Technologies) according to the manufacturer's instructions. The medium was changed every 2 days. Primary fibroblasts from an MDC1A patient (GM23311) and a control subject (GM23309) were purchased from Coriell Cell Repositories (Camden, NJ). The cells were grown in minimum essential medium with GlutaMAX (Life Technologies) supplemented with 10% fetal bovine serum (Life Technologies) at 37°C and 5% CO_2.

Proteasome Activity

Protein lysates were obtained by adding cell pellets into lysis buffer [50 mmol/L HEPES (pH 7.5), 5 mmol/L EDTA, 150 mmol/L NaCl, 1% CHAPS] on ice for 30 minutes with vortexing at 10-minute intervals. The lysates were centrifuged at 13,000 rpm (15,700 × *g*) for 15 minutes at 4°C, and the protein concentration in the supernatant was determined by the bicinchoninic acid method using a Pierce BCA protein assay kit (Thermo Fisher Scientific, Waltham, MA). Protein (25 ng) was added to substrate buffer (25 mmol/L HEPES at pH 7.5, 0.5 mmol/L EDTA, 0.05% NP-40, 0.001% SDS), and 20S proteasome activity was determined using a fluorometry-based microplate assay (Millipore, Billerica, MA) that detects

chymotrypsin-like activity by monitoring amido-4-methylcoumarin (AMC) release from the synthetic peptide substrate LLVY-AMC.

RNA Extraction, cDNA Synthesis, and qPCR for mRNA Detection

Total RNA was extracted from 10 mg of crushed quadriceps muscle from dy^{3K}/dy^{3K}, bortezomib-treated dy^{3K}/dy^{3K}, WT, and bortezomib-treated WT mice (3.5 weeks of age for untreated mice and 5.5 weeks for treated mice); from dy^{2J}/dy^{2J}, dy^{3K}δE3, and integrin α7−deficient mice and corresponding WT litter mates; from *mdx*, β-sarcoglycan−deficient, and C57BL/6 mice (5 to 7 weeks of age) and from cardiac muscle from dy^{3K}/dy^{3K} and WT litter mates (3.5 weeks of age). RNA was extracted using an RNeasy mini kit (Qiagen, Venlo, The Netherlands; Valencia, CA), with an initial step of proteinase K digestion (Fermentas; Thermo Fisher Scientific). Complementary DNA was synthesized from 1 μg of total RNA with random primers and SuperScript III Reverse Transcriptase (Life Technologies) according to the manufacturer's instructions. Amplification by quantitative real-time PCR (qPCR) was performed in a LightCycler 480 system (Roche Diagnostics, Indianapolis, IN) in 96-well plates with previously described primers for NF-κB-p65, FoxO1, MAFbx/atrogin-1, MuRF1, and ubiquitin.[40–42] Thermal cycling conditions were as follows: preincubation for 15 minutes at 95°C, then 40 cycles of 15 seconds at 94°C, 30 seconds at 55°C, and 30 seconds at 72°C, followed by a melting-curve cycle of 1 second at 95°C, 30 seconds at 65°C, and 0.11°C per second increase of temperature until 95°C.

Total RNA was extracted from human myoblasts using a High Pure RNA isolation kit (Roche Diagnostics), according to the manufacturer's instructions. First-strand cDNA was synthesized from total RNA (0.7 μg) with oligonucleotide dT15 primers and random primers p(dN)6 by using a First Strand cDNA synthesis kit (Roche Diagnostics). Primer sequences were designed and analyzed through Primer-BLAST version 2.0.13 (*http://www.ncbi.nlm.nih.gov/tools/primer-blast*) and the Operon tool (*http://www.operon.com/tools/oligo-analysis-tool.aspx*, both last accessed January 10, 2014) was used to check the putative primer−dimer formation. Oligonucleotide sequences (forward and reverse, respectively) were as follows: NF-κB-p65, 5′-CTGCCGGGATGGCTTCTAT-3′ and 5′-CCGCTTCTTCACACACTGGAT-3′ (NM_021975.3); 20S core particle subunit α2, 5′-ACCGAGAAAAAGCAGAAATCCA-3′ and 5′-ATGGACGAACACCACCTGAC-3′ (NM_002787.4); USP19, 5′-AGCGGCACAAGATGAGAAAT-3′ and 5′-ACGGGTCAAAAGTGATGGAG-3′ (NM_006677.1); ubiquitin, 5′-ATTTGGGTCGCGGTTCTTG-3′ and 5′-TGCCTTGACATTCTCGATGGT-3′[43]; and GAPDH, 5′-CAGTCAGCCGCATCTTCTTT-3′ and 5′-CCCAATACGACCAAATCCGTT-3′ (NM_002046.4). Amplification conditions were 45 cycles of 10 seconds at 96°C, 10 seconds at 60°C, and 10 seconds at 72°C.

Amplification curves were analyzed using the manufacturer's LightCycler 480 software version 1.5.0 (Roche Diagnostics), both for determination of C_T (by the second-derivative method) and for melting-curve analysis. Expression levels were calculated relative to the endogenous control genes *GAPDH* and/or *RPLP0* (alias *P0*)[42] and then relative to control samples.

RNA Isolation, cDNA Synthesis, and qPCR for miRNA Detection

Total RNA was extracted from quadriceps muscle snap-frozen in liquid nitrogen using a miRCURY RNA isolation kit (Exiqon, Vedbaek, Denmark; Woburn, MA) according to the manufacturer's instructions. Total RNA from cells was extracted using a commercial column-based system (miRNeasy mini kit; Qiagen) according to the manufacturer's instructions. RNA (20 ng) was reverse-transcribed using a miRCURY LNA universal RT cDNA synthesis kit (Exiqon). The cDNA was diluted 80 times and assayed in 10-μL PCR reactions according to the protocol for the miRCURY LNA universal RT microRNA PCR system. The amplification was performed in a LightCycler 480 qPCR system (Roche Diagnostics) in 96-well plates. The amplification curves were analyzed using the manufacturer's LightCycler software, both for determination of C_T (by the second-derivative method) and for melting-curve analysis. Primers for miR-1 and miR-133a were designed by Exiqon (product no. 204344 and 204788, respectively). We used U6 snRNA and let-7a as internal controls (product no. 203907 and 204775, respectively; Exiqon).

Histology and Immunofluorescence

Quadriceps and diaphragm muscles from dy^{3K}/dy^{3K}, bortezomib-treated dy^{3K}/dy^{3K}, WT, and bortezomib-treated WT mice were dissected after euthanasia and frozen in optimal cutting temperature compound (Tissue-Tek OCT; Sakura Finetek, Torrance, CA) in liquid nitrogen. Sections (7 μm thick) were stained with H&E, Masson's trichrome (using an HT15 commercial kit; Sigma-Aldrich, St. Louis, MO), or biotinylated wheat germ agglutinin, which was detected with fluorescein avidin D (Vector Laboratories, Burlingame, CA). Also, sections were processed for immunofluorescence analyses according to standard procedures with rat monoclonal anti−tenascin-C (Mtn15)[19] or mouse monoclonal anti−caspase-3 (BD Transduction Laboratories CPP32; BD Biosciences, San Jose, CA). Sections were analyzed and images captured with a Zeiss Axioplan fluorescence microscope (Carl Zeiss Microscopy, Jena, Germany) using an ORCA 1394 ER digital camera (Hamamatsu Photonics, Hamamatsu City, Japan) and Openlab software version 3 (Improvision, Coventry, UK).

Morphometric Analysis

Quantifications were performed on entire quadriceps and diaphragm muscle cross sections. H&E and Masson's

trichrome–stained sections were scanned using an Aperio ScanScope CS2 scanner with ScanScope console version 8.2.0.1263 (Aperio, Vista, CA). For tenascin-C labeled sections, low magnification (×2.5) Tiff-format images of whole muscle or multiple images at ×10 magnification covering the whole muscle were used. The area within muscle corresponding to Masson's trichrome–positive areas and to tenascin-C labeling was quantified relative to the entire area of the quadriceps cross section. The images of tenascin-C and Masson's trichrome staining were converted to 8-bit-mode images, and the measurements were set to a threshold that was manually adjusted for every individual image (the total muscle area versus stained area, measured in square pixels). The numbers of centrally located nuclei, caspase-3–positive cells, Masson's trichrome–positive areas, and tenascin-C–positive areas were quantified using ImageJ software version 1.43u (NIH, Bethesda, MD). The fiber area of biotinylated wheat germ agglutinin–stained muscle fibers was measured and quantified using Adobe Photoshop CS5 extended version (Adobe Systems, San Jose, CA).

Exploratory Locomotion Test

Exploratory locomotion was evaluated in an open-field test. In each experiment, a mouse was placed into a new cage and allowed to explore the cage for 5 minutes. The time that the mouse spent moving around was measured manually.

Statistical Analysis

Except as otherwise indicated, data were analyzed using one-way analysis of variance with a Tukey's multiple comparison test to determine differences between groups. *U*-test or Student's *t*-test was used for statistical analyses of gene expression. The statistical significance of relative expression changes of target miRNA levels was analyzed using one-way analysis of variance with Tukey's multiple comparison test for quadriceps muscle and REST 2009 software (*http://www.gene-quantification.info*, last accessed January 10, 2014) for myoblasts.[44] Finally, the log-rank test was used for the analysis of significance of survival curves. Statistical significance was accepted for $P < 0.05$.

Results

Increased Expression of Proteasome-Related Genes in Laminin α2 Chain–Deficient Muscle but Not in Other Mouse Models of Muscular Dystrophy

We have recently demonstrated enhanced expression of ubiquitin-proteasome–related genes in laminin α2 chain–deficient dy^{3K}/dy^{3K} skeletal muscle.[34] To elucidate whether the augmented expression is a feature of laminin α2 chain–deficient muscle or whether there is a general increase in expression of proteasome-related genes in muscular dystrophy, we analyzed the expression of the transcription factors NF-κB-p65 and FoxO1, the key ubiquitin ligases MuRF1 and atrogin-1, and finally ubiquitin mRNAs in quadriceps muscle from mice with different forms of muscular dystrophy. As previously shown,[44] we detected significantly increased levels of NF-κB-p65, FoxO1, MuRF, atrogin-1, and ubiquitin mRNAs in 3.5-week-old dy^{3K}/dy^{3K} quadriceps muscle (Supplemental Figure S1A). A similar increase was also detected in muscle from 5-week-old dy^{2J}/dy^{2J} mice (Supplemental Figure S1B), which exhibit a much milder muscle phenotype than dy^{3K}/dy^{3K} mice. Because of a mutation in the laminin N-terminal (LN) domain, there is slightly reduced expression of truncated laminin α2 chain devoid of the LN domain in dy^{2J}/dy^{2J} muscle. Nevertheless, these mice develop relatively mild muscular dystrophy and peripheral neuropathy.[45,46]

We next quantified the expression level of proteasome-related genes in quadriceps muscle from 5-week-old dystrophin-deficient *mdx* mice (a Duchenne muscular dystrophy mouse model) and 5-week-old β-sarcoglycan–deficient *Sgcb*-null mice (a limb-girdle muscular dystrophy type 2E mouse model).[38] No major modification in expression levels was detected in *mdx* or *Sgcb*-null ($Sgcb^{-/-}$) muscle (Supplemental Figure S1, C and D).

We next assessed quadriceps muscle from 5-week-old dy^{3K}δE3 mice. These laminin α2 chain–deficient mice overexpress a shortened laminin α1 chain devoid of the dystroglycan binding site; however, the integrin binding site remains uninterrupted. Accordingly, dy^{3K}δE3 limb muscles are quite dystrophic, but diaphragm and heart muscles are spared.[21] The expression of NF-κB-p65, FoxO1, MuRF1, atrogin-1, and ubiquitin mRNAs was not increased in dy^{3K}δE3 quadriceps muscle (Supplemental Figure S1E), suggesting that the laminin α2 chain receptor dystroglycan may not be involved in the downstream proteasome activity. To assess whether the expression of proteasome-related genes is altered when the other laminin α2 chain receptor, the integrin α7 subunit, is absent in skeletal muscle, we evaluated quadriceps muscle from integrin α7–deficient mice. At 5 weeks of age, integrin α7–deficient muscles are only very mildly dystrophic.[47] No major alteration in expression levels of proteasome-related genes was detected (Supplemental Figure S1F). Last, we determined the expression levels of proteasome-related genes in laminin α2 chain–deficient cardiac muscle, which appears to be relatively mildly affected both in laminin α2 chain–deficient mice and in MDC1A patients.[2] Only ubiquitin mRNA levels were significantly increased in dy^{3K}/dy^{3K} cardiac muscle (Supplemental Figure S1G).

Bortezomib Enhances Weight, Locomotion, and Survival of Laminin α2 Chain–Deficient Mice

We have previously demonstrated that short-term proteasome inhibition with MG-132 reduces disease manifestations in dystrophic dy^{3K}/dy^{3K} muscle.[34] In the present study, we determined the efficacy of the proteasome inhibitor bortezomib, a drug that is approved for the treatment of patients with multiple myeloma and mantle cell lymphoma.[36,37] In a

pilot study, 2.5-week-old dy^{3K}/dy^{3K} mice were injected intravenously with 0.8 mg/kg bortezomib (the dose given previously to *mdx* mice[48]). However, the bortezomib-treated dy^{3K}/dy^{3K} mice died a few days later, at approximately the same time as untreated dy^{3K}/dy^{3K} mice, whereas WT pups tolerated the dose. For the present study, therefore, we administered 0.4 mg/kg bortezomib (roughly corresponding to the dose given to patients with multiple myeloma) to dy^{3K}/dy^{3K} mice at 2.5 weeks of age. The great majority of animals survived, and a second injection was given at 3.5 weeks of age. It has previously been shown that the median survival of dy^{3K}/dy^{3K} mice is approximately 22 to 23 days, and most mice are dead by 4 weeks of age.[34] We analyzed mice and muscles at 14 days after the second injection (ie, at 5.5 weeks of age, when dy^{3K}/dy^{3K} mice would ordinarily be dead), and found that the expression of proteasome-related genes was partially normalized with the two bortezomib injections (Supplemental Figure S1H).

We first compared the overall health status of bortezomib-treated animals by investigating whether systemic bortezomib injections contributed to increased body weight, improved locomotion, and longer life span. Body weight was significantly increased, although bortezomib-treated dy^{3K}/dy^{3K} mice remained significantly smaller than WT mice (Figure 1A). Mice of the dy^{3K}/dy^{3K} strain have been shown to be significantly less active (compared with WT or heterozygous mice) in an exploratory locomotion test,[21] but in the present study bortezomib-treated dy^{3K}/dy^{3K} mice exhibited the same level of activity as WT mice (Figure 1B). Finally, the median survival of bortezomib-treated dy^{3K}/dy^{3K} mice was 32 days, a significant increase of 36% relative to the 22 to 23 days established as the median survival for this strain[34] (Figure 1C).

Bortezomib Partially Improves Muscle Morphology and Reduces Apoptosis and Fibrosis in Laminin α2 Chain–Deficient Muscle

By morphometric measurement, we evaluated muscle fiber cross-sectional area, central nucleation, apoptosis, and fibrosis, all of which are affected in laminin α2 chain–deficient muscles[16] (Figure 2, Figure 3, and Supplemental Figure S2). The muscle fiber cross-sectional area was significantly increased in quadriceps muscle in bortezomib-treated mice (Figure 2B), and bortezomib also shifted fiber-size distribution toward the values of WT muscle (Figure 2C). Most WT fibers had cross-sectional areas from 500 to 1000 μm^2, and in this group of fibers there was no significant difference between WT and bortezomib-treated dy^{3K}/dy^{3K} muscle. However, there were significantly more small fibers (1 to 500 μm^2) in bortezomib-treated dy^{3K}/dy^{3K} muscle than in WT muscle. Also, the proportion of fibers in the 1000 to 1500 μm^2 group was significantly lower in bortezomib-treated dy^{3K}/dy^{3K} muscle than in WT muscle. Importantly, in each group of fibers there was always a significant difference between dy^{3K}/dy^{3K} muscle and bortezomib-treated dy^{3K}/dy^{3K} muscle. In addition, bortezomib slightly increased the fiber cross-sectional area in diaphragm muscle, but the difference was not significant (Supplemental Figure S2, B and C). By contrast, the average muscle fiber cross-sectional area was significantly reduced in dy^{3K}/dy^{3K} quadriceps (Figure 2B) and diaphragm (Supplemental Figure S2B) muscle, compared with WT or bortezomib-treated WT muscle. Also, an increased number of fibers with centrally located nuclei is evident in dy^{3K}/dy^{3K} muscle, indicating ongoing degeneration–regeneration processes (Figure 3A and Supplemental Figure S2D). However, central nucleation was not affected by bortezomib treatment, neither in quadriceps (Figure 3A) nor in diaphragm (Supplemental Figure S2D) muscle.

It is well established that apoptosis contributes to disease progression in MDC1A,[27] and we have previously demonstrated significantly increased number of procaspase-3/caspase-3–positive fibers in dy^{3K}/dy^{3K} quadriceps muscle (Figure 3B).[34,35] In bortezomib-treated animals, there were significantly fewer procaspase-3/caspase-3–positive muscle fibers in quadriceps muscle (Figure 3B). In diaphragm muscle, bortezomib to some extent reduced the proportion of procaspase-3/caspase-3–positive muscle fibers (from 19% to 15%), but the difference was not significant (Supplemental Figure S2E).

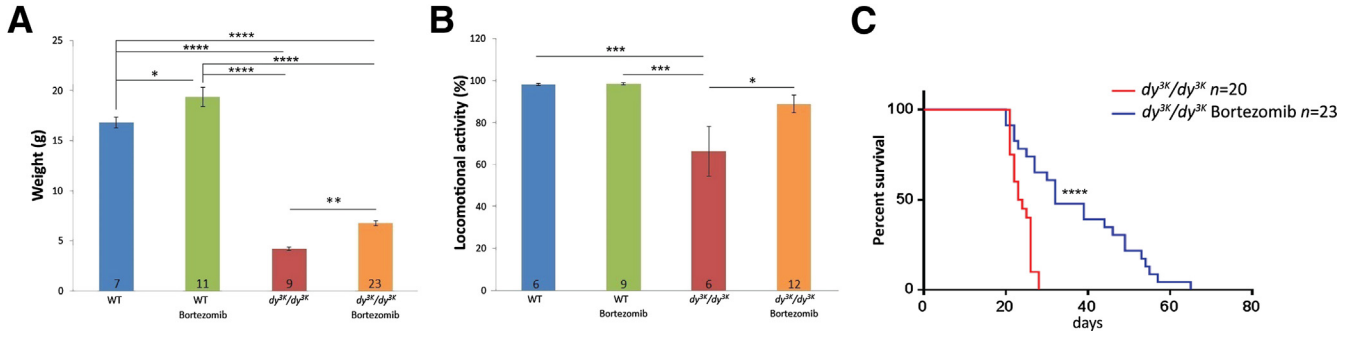

Figure 1 Bortezomib improves body weight, locomotion, and life span in dy^{3K}/dy^{3K} mice. **A:** Bortezomib treatment increased the body weight of dy^{3K}/dy^{3K} mice by approximately 3.5 g; however, bortezomib-treated mice remained significantly smaller than WT mice. **B:** Administration of bortezomib increased exploratory locomotion of dy^{3K}/dy^{3K} mice in an open-field test to WT levels. **C:** Bortezomib treatment increased survival in dy^{3K}/dy^{3K} mice. Median survival for noninjected dy^{3K}/dy^{3K} mice was 23.5 days, compared with 32 days for bortezomib-treated animals. Data are expressed as means ± SEM. $n = 6$ to 23, as indicated on data bars. $^*P < 0.05$, $^{***}P < 0.001$, and $^{****}P < 0.0001$.

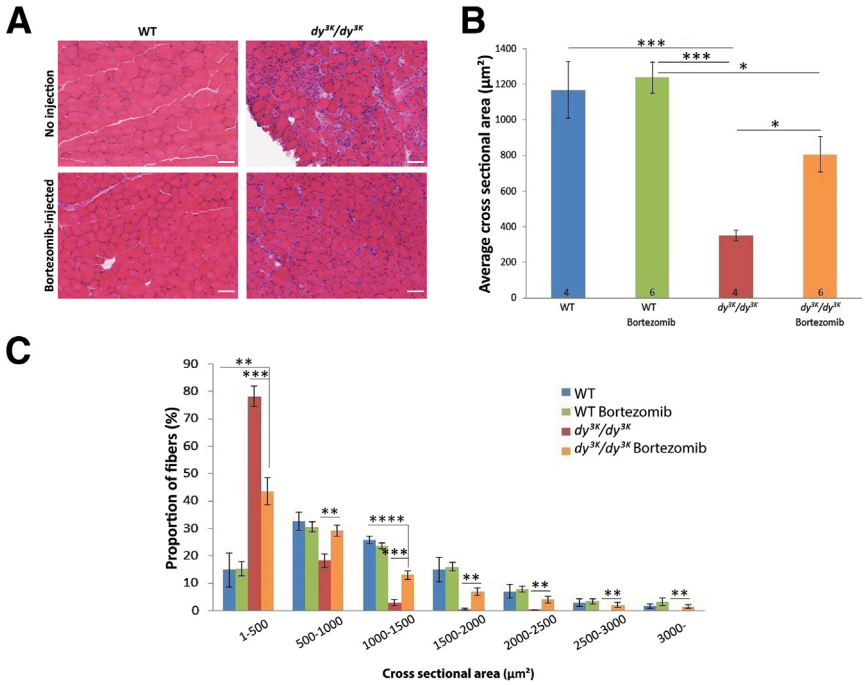

Figure 2 Bortezomib increases muscle fiber cross-sectional area in dy^{3K}/dy^{3K} quadriceps muscle. **A:** H&E staining of cross sections of quadriceps muscle from WT, bortezomib-treated WT, dy^{3K}/dy^{3K}, and bortezomib-treated dy^{3K}/dy^{3K} mice. **B:** Average muscle fiber cross-sectional area was reduced in quadriceps muscle of the dy^{3K}/dy^{3K} strain, mice, but it increased with bortezomib treatment. **C:** Bortezomib shifted fiber-size distribution toward the values of WT quadriceps muscle. Data are expressed as means ± SEM. $n = 4$ or 6, as indicated on data bars. $^{*}P < 0.05$, $^{**}P < 0.01$, $^{***}P < 0.001$, and $^{****}P < 0.0001$. Scale bar = 50 µm (**A**).

Laminin α2 chain–deficient muscles are also characterized by extensive fibrosis.[19,32,49] Masson's trichrome staining revealed a major replacement of muscle tissue with connective tissue in untreated dy^{3K}/dy^{3K} quadriceps muscle, whereas bortezomib-treated mice exhibited less fibrosis (Figure 3, C and D). As an independent measure of fibrosis, we also quantified tenascin-C expression, which has been shown to be significantly increased in dy^{3K}/dy^{3K} muscle.[19] Bortezomib administration resulted in less tenascin-C expression in quadriceps muscle of dy^{3K}/dy^{3K} mice (Figure 3, E and F). Bortezomib also mildly reduced fibrosis in dy^{3K}/dy^{3K} diaphragm muscle, but the difference was not significant (Supplemental Figure S2, F–G). Taken together, these findings provide evidence that bortezomib improves several histological hallmarks of disease in quadriceps muscle and, to a lesser extent, in diaphragm muscle.

It is also important to note that bortezomib treatment did not influence muscle architecture, activity, or survival of WT animals. Furthermore, plasma levels of cystatin-C were not increased, indicating that bortezomib does not cause decreased kidney function in dy^{3K}/dy^{3K} or WT mice (data not shown). Finally, we have previously shown that the proteasome inhibitor MG-132 does not appreciably improve the pathology of the peripheral nerve.[34] Bortezomib-treated dy^{3K}/dy^{3K} animals exhibited transient hind-leg paralysis, but it was not more severe than the transient paralysis detected in nontreated dy^{3K}/dy^{3K} mice (data not shown).

Bortezomib Partially Normalizes miR-1 and miR-133a Expression

Next, we characterized the expression of miRNAs that are promising disease biomarkers in muscular dystrophy. For example, it has been suggested that miR-1 and miR-133 can be considered as exploratory biomarkers for monitoring progression of muscle weakness and indirectly the remaining muscle mass in muscular dystrophy,[50] and expression of the muscle-specific miR-1 and miR-133a has been shown to be down-regulated in *mdx* muscle.[51] The expression profile of these miRNAs in MDC1A has not been investigated previously. In the present study, expression levels of miR-1 and miR-133a were significantly reduced in dy^{3K}/dy^{3K} quadriceps muscle (Figure 4A) and in MDC1A myoblasts (Figure 4B). Importantly, bortezomib treatment in mice significantly increased expression levels of miR-1 and miR-133a (Figure 4A).

Taken together, these findings show that the beneficial effects of bortezomib on muscle histology are sufficient to improve life span and activity of dy^{3K}/dy^{3K} mice. Also, for the first time, we have demonstrated altered miRNA expression in laminin α2 chain–deficient muscle that is partially normalized by bortezomib administration.

Effects of Bortezomib in MDC1A Primary Muscle Cells

To assess whether experimental findings in mice correlate with human biology, we investigated the expression of proteasome-related genes and proteasome activity in human laminin α2 chain–deficient myoblasts and myotubes. We detected increased expression of NF-κB-p65, ubiquitin, and the 20S core particle subunit α2 mRNAs in MDC1A myoblasts (Figure 5A). Also, expression of USP19 mRNA, which encodes a deubiquitinating enzyme with increased expression in atrophying skeletal muscle,[52] was enhanced in MDC1A myoblasts. Furthermore, proteasome activity was significantly augmented in MDC1A myoblasts (Figure 5B) and myotubes (Figure 5C). Taken together, these findings

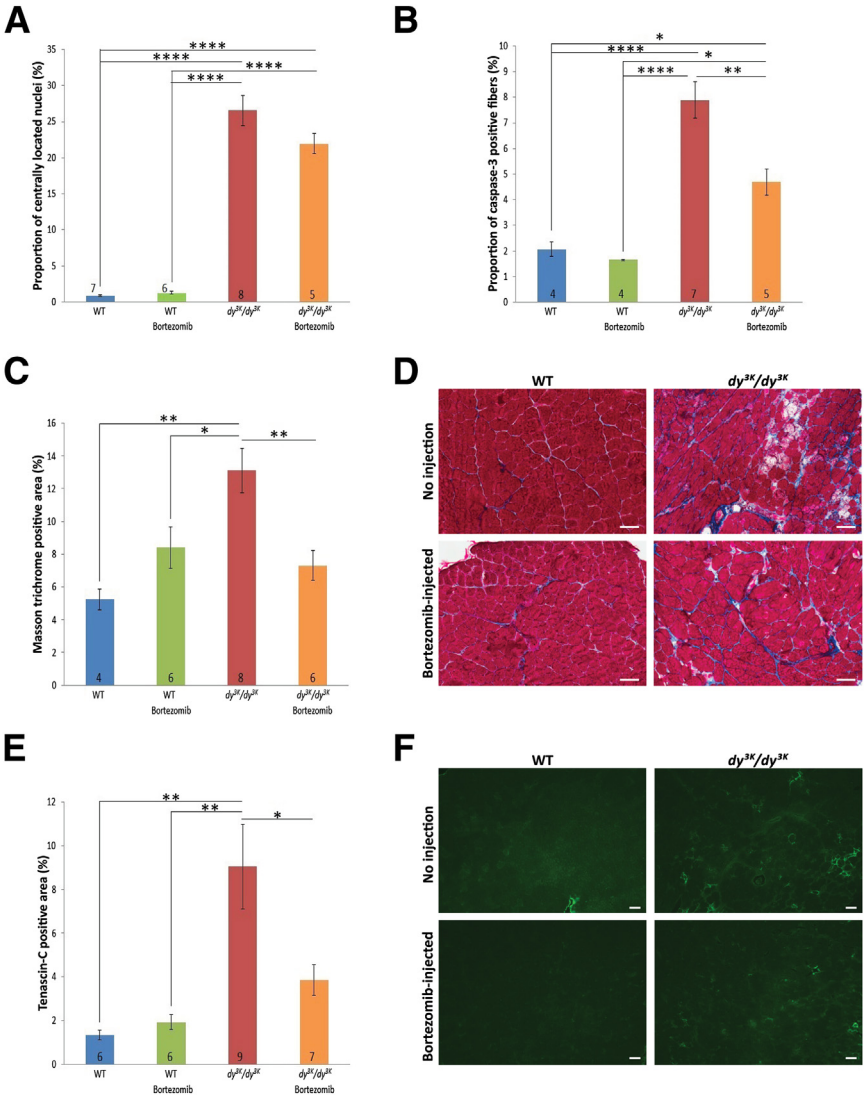

Figure 3 Bortezomib decreases apoptosis and fibrosis in dy^{3K}/dy^{3K} quadriceps muscle. **A:** The proportion of fibers with centrally located nuclei increased in dy^{3K}/dy^{3K} quadriceps muscle and was not significantly affected by bortezomib. **B:** Immunostaining using antibodies against procaspase-3/caspase-3 isoforms revealed an increased number of apoptotic fibers in dy^{3K}/dy^{3K} quadriceps muscle, which decreased with bortezomib treatment. **C** and **D:** Masson's trichrome staining of transverse cryosections of dy^{3K}/dy^{3K} quadriceps muscle revealed reduced collagen content with bortezomib treatment. **E** and **F:** In transverse cryosections of quadriceps muscle stained with antibodies against tenascin-C, bortezomib reduced the tenascin-C–positive area. Data are expressed as means ± SEM. $n = 5$ to 9, as indicated on data bars. $^{*}P < 0.05$, $^{**}P < 0.01$, and $^{****}P < 0.0001$. Scale bar = 50 μm (**D** and **F**).

suggest that increased proteasome activity is a characteristic of laminin α2 chain–deficient human muscle cells.

Having established that bortezomib partially alleviates muscle pathology in dy^{3K}/dy^{3K} mice, we next investigated whether bortezomib has beneficial effects on human laminin α2 chain–deficient muscle cells *in vitro*. Muscle cells were treated with 1 or 10 nmol/L bortezomib, followed by assessment of proteasome activity. Bortezomib significantly reduced proteasome activity in both myoblasts (Figure 5B) and myotubes (Figure 5C). Last, to investigate whether proteasome activity is also increased in other MDC1A cell types, we analyzed MDC1A fibroblasts. In contrast to MDC1A muscle cells, proteasome activity was not significantly altered in MDC1A fibroblasts (Supplemental Figure S3).

Discussion

Numerous approaches have been used to ameliorate MDC1A in different mouse models of the disease. Some of the transgenic approaches, including re-expression of laminin α2 chain in muscle or widespread overexpression of laminin α1 chain, result in near-complete muscle restoration.[19–23] The various pharmacological lines of attack, however, result in only partial recovery,[29,30,32,34,35] and only a few of the pharmacological compounds used (eg, doxycycline and losartan) have been approved by the U.S. Food and Drug Administration and similar counterparts in Europe, and even then the approval is not for muscular dystrophy. Thus, new pharmacological approaches should continue to be explored. We recently demonstrated that increased proteasome activity is pathogenic and that systemic administration of the proteasome inhibitor MG-132 significantly improves laminin α2 chain–deficient muscle and increases the life span in dy^{3K}/dy^{3K} mice.[34] However, MG-132 also inhibits calpains, however, and it is not suitable as a therapeutic compound in humans.[36] We therefore evaluated the use of the selective and therapeutic proteasome inhibitor bortezomib in a mouse model of MDC1A.

Here, we have provided evidence that bortezomib partially reduces many of the pathological symptoms in the

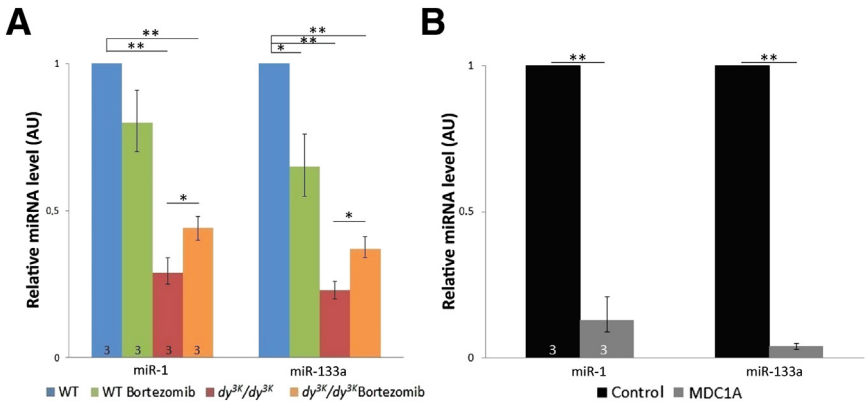

Figure 4 Expression of muscle-specific miR-1 and miR-133a is significantly down-regulated in laminin α2 chain–deficient muscle and partially corrected on administration of bortezomib. **A:** qPCR data revealed significantly down-regulated expression of muscle-specific miR-1 and miR-133a in dystrophic muscle of dy^{3K}/dy^{3K} mice, compared with WT muscle, which was partially increased after administration of bortezomib. **B:** miR-1 and miR-133a expression was also decreased in MDC1A myoblasts. Cells obtained from MDC1A patients were cultured *in vitro* and the expression of indicated miRNAs was analyzed by qPCR. Data are expressed as means ± SEM. $n = 3$, as indicated on data bars. $^{*}P < 0.05$, $^{**}P < 0.01$.

dy^{3K}/dy^{3K} mouse model of MDC1A. The benefits of the treatment encompassed increased life span and enhanced locomotive activity, coupled with increased muscle cross-sectional area, decreased apoptosis, reduced fibrosis, and partial normalization of miR-1 and miR-133a expression in quadriceps muscle. We also analyzed diaphragm muscle, because respiratory distress is one of the clinical symptoms of MDC1A; however, diaphragm muscle in bortezomib-treated mice exhibited only very limited reduction in pathology. Although it is problematic to evaluate studies performed in different laboratories and using different mouse models of MDC1A, it is clear that in most studies diaphragm muscles were not analyzed in great detail after various pharmacological approaches or that only some of the parameters were improved.[30–32,34,35,53] Nevertheless, the limitation with respect to diaphragm improvement must be taken into account in any consideration of proteasome inhibition as a potential MDC1A treatment.

It has been argued that inhibition of proteasomal degradation is likely to lead to severe adverse effects and that therefore administration of proteasome inhibitors may not constitute a good treatment option for MDC1A.[32] Because it induces apoptosis in a wide spectrum of tumor cells,[54] bortezomib could be counterproductive in MDC1A, given the increased incidence of apoptosis in this disease.[27] Although we are well aware of predominant toxicities reported in humans,[55] we stress that just two doses of bortezomib at 0.4 mg/kg significantly improved MDC1A pathology; more importantly, bortezomib reduced apoptosis in dy^{3K}/dy^{3K} muscle. Furthermore, there were no major adverse effects in WT animals, and bortezomib also reduced the proteasome activity in laminin α2 chain–deficient human cells (although we analyzed only one pair each of MDC1A and control myoblasts and fibroblasts). Thus, it could well be that MDC1A patients would benefit from a less frequent administration schedule than that of the treatment regimen for multiple myeloma and mantle cell lymphoma. Furthermore, new proteasome inhibitors have been developed, with improved adverse effect profiles.[56]

Even though bortezomib does not target the primary genetic cause of the disease and thus cannot entirely cure MDC1A, proteasome inhibition could still offer a supportive therapy that counteracts some of the pathological features in MDC1A. Interestingly, it was recently demonstrated that bortezomib administration into dystrophin-deficient golden retriever muscular dystrophy dogs at 4 months of age (when clinical signs of muscular dystrophy is already apparent in this model) reduced the level of phosphorylated NF-κB and decreased the amount of fibrosis in skeletal

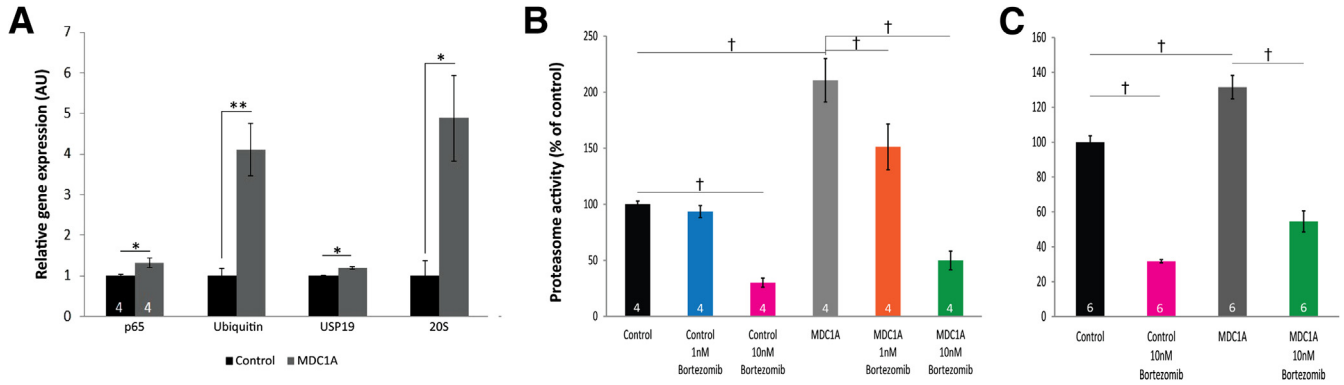

Figure 5 Bortezomib reduces proteasome activity in MDC1A muscle cells. **A:** Expression of NF-κB-p65, ubiquitin, 20S core particle subunit α2, and USP19 mRNAs increased in MDC1A myoblasts. **B:** Proteasome activity was significantly increased in MDC1A myoblasts and was reduced after administration of 1 and 10 nmol/L bortezomib. **C:** Proteasome activity was significantly increased in MDC1A myotubes and was reduced after administration of 10 nmol/L bortezomib. $^{*}P < 0.05$, $^{**}P < 0.01$; $^{\dagger}P < 0.01$ versus *U*-test after Krusakal-Wallis test. $n = 4$ or 6, as indicated on data bars.

muscle.[57] Although the main clinical signs related to muscular dystrophy persisted, it would be interesting to know whether bortezomib reduces clinical signs if treatment is initiated before onset of disease. Also, dy^{3K}/dy^{3K} mice might benefit even more from an earlier intervention than the 2.5 weeks of age we used. At this age, dy^{3K}/dy^{3K} mice are well into disease manifestations, which start at approximately 7 days of age with robust signs of inflammation.[58]

Neither dystrophin-deficient nor β-sarcoglycan−deficient mice exhibited a general up-regulation of the proteasome-related genes in skeletal muscle. However, it should be noted that expression of phosphorylated NF-κB-p65 is increased in dystrophin-deficient *mdx* mice; more importantly, it has been demonstrated that a reduction in NF-κB signaling improves muscle pathology in *mdx* mice.[59] Also, proteasome inhibition with MG-132 has shown some beneficial effects in dystrophin-deficient *mdx* mice,[60−62] although it was recently questioned whether proteasome inhibition actually reduced the severity of muscle dysfunction.[63] Nevertheless, increased expression of members of the dystrophin−glycoprotein complex after proteasome inhibition has been reported in dystrophin-deficient mice, and this salvation from degradation could be therapeutically beneficial.[60−62] Likewise, proteasome inhibition re-established the biological function of missense-mutated dysferlin in muscle cells derived from patients.[64] Thus, it would be interesting to evaluate proteasome inhibition in sarcoglycan-deficient-mice as well.

The connection between laminin α2 chain-deficiency and increased proteasome and autophagy activity has not yet been elucidated. Both proteasomal degradation and autophagy are suppressed by PI3K/Akt,[65] and we have previously shown that Akt phosphorylation is reduced in dy^{3K}/dy^{3K} muscle.[34,35] Laminin α2 chain binds mainly to integrin α7β1 and dystroglycan in skeletal muscle.[7,8] There is a secondary reduction of integrin α7 chain in dy^{3K}/dy^{3K} muscle,[13] and therefore absence of laminin α2 chain and integrin α7 subunit could lead to reduced Akt activation. Also, disruption of laminin−dystroglycan interaction results in decreased phosphorylation of Akt, at least in muscle cells *in vitro*.[66] We have not analyzed whether Akt is underphosphorylated in dy^{3K}δE3 muscle, but neither proteasome-related nor autophagy-related genes were up-regulated in dy^{3K}δE3 muscle, despite disrupted laminin−dystroglycan interactions.[35] The expression of proteasome-related genes was unaltered also in integrin α7−deficient muscle. Thus, the gene expression data suggest that neither dystroglycan nor integrin α7β1 is involved in the downstream proteasome activity. The relationship between deficiency of laminin α2 chain (and laminin α2 chain receptors) and increased proteasome activity, as well as enhanced autophagy, remains to be determined.

In summary, we have demonstrated that bortezomib, a proteasome inhibitor already in clinical use, improves the muscle phenotype and life span of laminin α2 chain−deficient dy^{3K}/dy^{3K} mice and reduces proteasome activity in MDC1A muscle cells. It cannot be assured that bortezomib will have the same advantageous effects in humans as it has in mice, but our results suggest that it may be worth testing bortezomib as a possible supportive therapy for MDC1A.

Acknowledgments

We thank Valérie Allamand for providing the human cells and Kinga Gawlik for expert technical help.

Supplemental Data

Supplemental material for this article can be found at *http://dx.doi.org/10.1016/j.ajpath.2014.01.019*.

References

1. Allamand V, Guicheney P: Merosin-deficient muscular dystrophy, autosomal recessive (MDC1A, MIM#156225, LAMA2 gene coding for α2 chain of laminin). Eur J Hum Genet 2002, 10:91−94
2. Voit T, Tomé FMS: The congenital muscular dystrophies. Edited by Angel AG, Franzini-Armstrong C. In Myology: Basic and Clinical. vol 2, ed 3. New York, McGraw-Hill, 2004, pp 1203−1238
3. Leivo I, Engvall E: Merosin, a protein specific for basement membranes of Schwann cells, striated muscle, and trophoblast, is expressed late in nerve and muscle development. Proc Natl Acad Sci USA 1988, 85:1544−1588
4. Xu H, Christmas P, Wu XR, Wewer UM, Engvall E: Defective muscle basement membrane and lack of M-laminin in the dystrophic dy/dy mouse. Proc Natl Acad Sci USA 1994, 91:5572−5576
5. Helbling-Leclerc A, Zhang X, Topaloglu H, Cruaud C, Tesson F, Weissenbach J, Tomé FMS, Schwartz K, Fardeau M, Tryggvason K, Guicheney P: Mutations in the laminin α2 chain gene (LAMA2) cause merosin-deficient muscular dystrophy. Nat Genet 1995, 11: 216−218
6. Ibraghimov-Beskrovnaya O, Ervasti JM, Leveille CJ, Slaughter CA, Sernett SW, Campbell KP: Primary structure of dystrophin-associated glycoproteins linking dystrophin to the extracellular matrix. Nature 1992, 355:696−702
7. Talts JF, Andac Z, Gohring W, Brancaccio A, Timpl R: Binding of the G domains of laminin α1 and α2 chains and perlecan to heparin, sulfatides, α-dystroglycan and several extracellular matrix proteins. EMBO J 1999, 18:863−870
8. von der Mark H, Williams I, Wendler O, Sorokin L, von der Mark K, Pöschl E: Alternative splice variants of α7β1 integrin selectively recognize different laminin isoforms. J Biol Chem 2002, 277:6012−6016
9. Ervasti JM, Campbell KP: A role for the dystrophin-glycoprotein complex as a transmembrane linker between laminin and actin. J Cell Biol 1993, 122:809−823
10. Petrof BJ, Shrager JB, Stedman HH, Kelly AM, Sweeney HL: Dystrophin protects the sarcolemma from stresses developed during muscle contraction. Proc Natl Acad Sci USA 1993, 90: 3710−3714
11. Vachon PH, Xu H, Liu L, Loechel F, Hayashi Y, Arahata K, Reed JC, Wewer UM, Engvall E: Integrins (α7β1) in muscle function and survival. Disrupted expression in merosin-deficient congenital muscular dystrophy. J Clin Invest 1997, 10:1870−1881
12. Moll J, Barzaghi P, Lin S, Bezakova G, Lochmüller H, Engvall E, Müller U, Rüegg MA: An agrin minigene rescues dystrophic symptoms in a mouse model for congenital muscular dystrophy. Nature 2001, 413:302−307
13. Gawlik KI, Mayer U, Blomberg K, Sonnenberg A, Ekblom P, Durbeej M: Laminin α1 chain mediated reduction of laminin α2 chain deficient muscular dystrophy involves integrin α7β1 and dystroglycan. FEBS Lett 2006, 580:1759−1765

14. Kuang W, Xu H, Vilquin JT, Engvall E: Activation of the Lama2 gene in muscle regeneration: abortive regeneration in laminin α2-deficiency. Lab Invest 1999, 79:1601–1613
15. Hayashi YK, Tezak Z, Momoi T, Nonaka I, Garcia CA, Hoffman EP, Arahata K: Massive muscle cell degeneration in the early stage of merosin-deficient congenital muscular dystrophy. Neuromuscul Disord 2001, 11:350–359
16. Gawlik KI, Durbeej M: Skeletal muscle laminin and MDC1A: pathogenesis and treatment strategies. Skelet Muscle 2011, 1:9
17. Miyagoe Y, Hanaoka K, Nonaka I, Hayasaka M, Nabeshima Y, Arahata K, Nabeshima Y, Takeda S: Laminin α2 chain-null mutant mice by targeted disruption of the Lama2 gene: a new model of merosin (laminin 2)-deficient congenital muscular dystrophy. FEBS Lett 1997, 415:33–39
18. Guo LT, Zhang XU, Kuang W, Xu H, Liu LA, Vilquin JT, Miyagoe-Suzuki Y, Takeda S, Rüegg MA, Wewer UM, Engvall E: Laminin α2 deficiency and muscular dystrophy; genotype-phenotype correlation in mutant mice. Neuromuscul Disord 2003, 3:207–215
19. Gawlik K, Miyagoe-Suzuki Y, Ekblom P, Takeda S, Durbeej M: Laminin α1 chain reduces muscular dystrophy in laminin α2 chain deficient mice. Hum Mol Genet 2004, 13:1775–1784
20. Gawlik KI, Li JY, Petersén Å, Durbeej M: Laminin α1 chain improves laminin α2 chain deficient neuropathy. Hum Mol Genet 2006, 15:2690–2700
21. Gawlik KI, Åkerlund M, Carmignac V, Elamaa H, Durbeej M: Distinct roles for laminin globular domains in laminin α1 chain mediated rescue of murine laminin α2 chain deficiency. PLoS One 2010, 5:e11549
22. Gawlik KI, Durbeej M: Transgenic overexpression of laminin α1 chain in laminin α2 chain-deficient mice rescues the disease throughout the lifespan. Muscle Nerve 2010, 42:30–37
23. Kuang W, Xu H, Vachon PH, Engvall E: Merosin-deficient congenital muscular dystrophy. Partial genetic correction in two mouse models [Erratum appeared in J Clin Invest 1998, 102(6): following 1275]. J Clin Invest 1998, 102:844–852
24. Bentzinger CF, Barzaghi P, Lin S, Rüegg MA: Overexpression of miniagrin in skeletal muscle increases muscle integrity and regenerative capacity in laminin-α2-deficient mice. FASEB J 2005, 19:934–942
25. Meinen S, Barzaghi P, Lin S, Lochmüller H, Rüegg MA: Linker molecules between laminins and dystroglycan ameliorate laminin-α2-deficient muscular dystrophy at all disease stages. J Cell Biol 2007, 176:979–993
26. Doe JA, Wuebbles RD, Allred ET, Rooney JE, Elorza M, Burkin DJ: Transgenic overexpression of the α7 integrin reduces muscle pathology and improves viability in the dy(W) mouse model of merosin-deficient congenital muscular dystrophy type 1A. J Cell Sci 2011, 124:2287–2297
27. Girgenrath M, Dominov JA, Kostek CA, Miller JB: Inhibition of apoptosis improves outcome in a model of congenital muscular dystrophy. J Clin Invest 2004, 114:1635–1639
28. Kumar A, Yamauchi J, Girgenrath T, Girgenrath M: Muscle-specific expression of insulin-like growth factor 1 improves outcome in Lama2Dy-w mice, a model for congenital muscular dystrophy type 1A. Hum Mol Genet 2011, 20:2333–2343
29. Erb M, Meinen S, Barzaghi P, Sumanovski LT, Courdier-Früh I, Rüegg MA, Meier T: Omigapil ameliorates the pathology of muscle dystrophy caused by laminin-α2 deficiency. J Pharmacol Exp Ther 2009, 331:787–795
30. Girgenrath M, Beermann ML, Vishnudas VK, Homma S, Miller JB: Pathology is alleviated by doxycycline in a laminin-α2-null model of congenital muscular dystrophy. Ann Neurol 2009, 65:47–56
31. Elbaz M, Yanay N, Aga-Mizrachi S, Brunschwig Z, Kassis I, Ettinger K, Barak V, Nevo Y: Losartan, a therapeutic candidate in congenital muscular dystrophy: studies in the dy^{2J}/dy^{2J} mouse. Ann Neurol 2012, 71:699–708
32. Meinen S, Lin S, Rüegg MA: Angiotensin II type 1 receptor antagonists alleviate muscle pathology in the mouse model for laminin-α2-deficient congenital muscular dystrophy (MDC1A). Skelet Muscle 2012, 2:18
33. Rooney JE, Knapp JR, Hodges BL, Wuebbles RD, Burkin DJ: Laminin-111 protein therapy reduces muscle pathology and improves viability of a mouse model of merosin-deficient congenital muscular dystrophy. Am J Pathol 2012, 180:1593–1602
34. Carmignac V, Quéré R, Durbeej M: Proteasome inhibition improves the muscle of laminin α2 chain-deficient mice. Hum Mol Genet 2011, 20:541–552
35. Carmignac V, Svensson M, Körner Z, Elowsson L, Matsumura C, Gawlik K, Allamand V, Durbeej M: Autophagy is increased in laminin α2 chain-deficient muscle and inhibition improves muscle morphology in a mouse model of MDC1A. Hum Mol Genet 2011, 20:4891–4902
36. Goldberg AL: Development of proteasome inhibitors as research tools and cancer drugs. J Cell Biol 2012, 199:583–588
37. Buac D, Shen M, Schmitt S, Kona FR, Deshmukh R, Zhang Z, Neslund-Dudas C, Mitra B, Dou QP: From bortezomib to other inhibitors of the proteasome and beyond. Curr Pharm Des 2013, 19:4025–4038
38. Durbeej M, Cohn RD, Hrstka RF, Moore SA, Allamand V, Davidson BL, Williamson RA, Campbell KP: Disruption of the β-sarcoglycan gene reveals pathogenetic complexity of limb-girdle muscular dystrophy type 2E. Mol Cell 2000, 5:141–151
39. Allamand V, Bidou L, Arakawa M, Floquet C, Shiozuka M, Paturneau-Jouas M, Gartioux C, Butler-Browne GS, Mouly V, Rousset JP, Matsuda R, Ikeda D, Guicheney P: Drug-induced readthrough of premature stop codons leads to the stabilization of laminin α2 chain mRNA in CMD myotubes. J Gene Med 2008, 10:217–224
40. Mammucari C, Milan G, Romanello V, Masiero E, Rudolf R, Del Piccolo P, Burden SJ, Di Lisi R, Sandri C, Zhao J, Goldberg A, Schiaffino S, Sandri M: FoxO3 controls autophagy in skeletal muscle in vivo. Cell Metab 2007, 6:458–471
41. Laure L, Danièle N, Suel L, Marchand S, Aubert S, Bourg N, Roudauc C, Dugez S, Bartoli M, Richard I: A new pathway encompassing calpain 3 and its newly identified substrate cardiac ankyrin repeat protein is involved in the regulation of the nuclear factor κB pathway in skeletal muscle. FEBS J 2010, 277:4322–4337
42. Fontes-Oliveira CC, Busquets S, Toledo M, Penna F, Paz Aylwin M, Sirisi S, Silva AP, Orpí M, García A, Sette A, Inês Genovese M, Olivan M, López-Soriano F, Argilés JM: Mitochondrial and sarcoplasmic reticulum abnormalities in cancer cachexia: altered energetic efficiency? Biochim Biophys Acta 2013, 1830:2770–2778
43. Vandesompele J, De Preter K, Pattyn F, Poppe B, Van Roy N, De Paepe A, Speleman F: Accurate normalization of real-time quantitative RT-PCR data by geometric averaging of multiple internal control genes. Genome Biol 2002, 3. RESEARCH0034
44. Pfaffl MW, Horgan GW, Dempfle L: Relative expression software tool (REST) for group-wise comparison and statistical analysis of relative expression results in real-time PCR. Nucleic Acids Res 2002, 30:e36
45. Xu H, Wu XR, Wewer UM, Engvall E: Murine muscular dystrophy caused by a mutation in the laminin α2 (Lama2) gene. Nat Genet 1994, 8:297–302
46. Sunada Y, Bernier SM, Utani A, Yamada Y, Campbell KP: Identification of a novel mutant transcript of laminin α2 chain gene responsible for muscular dystrophy and dysmyelination in dy2J mice. Hum Mol Genet 1995, 4:1055–1061
47. Welser JV, Rooney JE, Cohen NC, Gurpur PB, Singer CA, Evans RA, Haines BA, Burkin DJ: Myotendinous junction defects and reduced force transmission in mice that lack α7 integrin and utrophin. Am J Pathol 2009, 175:1545–1554
48. Gazzerro E, Assereteo S, Bonetto A, Sotiga F, Scarfi S, Pistorio A, Bonuccelli G, Cilli M, Bruno C, Zara F, Lisanti MP, Minetti C: Therapeutic potential of proteasome inhibition in Duchenne and Becker muscular dystrophies. Am J Pathol 2010, 176:1863–1877
49. Taniguchi M, Kurahashi H, Noguchi S, Sese J, Okinaga T, Tsukahara T, Guicheney P, Ozono K, Nishino I, Morishita S, Toda T: Expression profiling of muscles from Fukuyama-type congenital

muscular dystrophy and laminin α2 deficient congenital muscular dystrophy; is congenital muscular dystrophy a primary fibrotic disease? Biochem Biophys Res Commun 2006, 342:489–502
50. Zaharieva IT, Calissano M, Scoto M, Preston M, Cirak S, Feng L, Collins J, Kole R, Guglieri M, Straub V, Bushby K, Ferlini A, Morgan JE, Muntoni FP: Dystromirs as serum biomarkers for monitoring the disease severity in Duchenne muscular dystrophy. PLoS One 2013, 8:e80263
51. Roberts TC, Blomberg KE, McClorey G, El Andaloussi S, Godfrey C, Betts C, Coursindel T, Gait MJ, Smith CI, Wood MJ: Expression analysis in multiple muscle groups and serum reveals complexity in the microRNA transcriptome of the mdx mouse with implications for therapy. Mol Ther Nucleic Acids 2012, 1:e39
52. Combaret L, Olasunkanmi AJA, Bedard N, Baracos V, Attaix D, Wing SS: USP19 is a ubiquitin-specific protease regulated in rat skeletal muscle during catabolic states. Am J Physiol Endocrinol Metab 2005, 288:E693–E700
53. Meinen S, Lin S, Thurnherr R, Erb M, Meier T, Rüegg MA: Apoptosis inhibitors and mini-agrin have additive benefits in congenital muscular dystrophy mice. EMBO Mol Med 2011, 3:465–479
54. Almond JB, Cohen GM: The proteasome: a novel target for cancer chemotherapy. Leukemia 2002, 16:433–443
55. Menashe J: Managing and avoiding bortezomib toxicity. Community Oncol 2007, 4:480–484
56. Kortuem KM, Stewart AK: Carfilzomib. Blood 2013, 121:893–897
57. Araujo KP, Bonuccelli G, Duarte CN, Gaiad TP, Moreira DF, Feder D, Belizario JE, Miglino MA, Lisanti MP, Ambrosio CE: Bortezomib (PS-341) treatment decreases inflammation and partially rescues the expression of the dystrophin-glycoprotein complex in GRMD dogs. PLoS One 2013, 8:e61367
58. Gawlik KI, Holmberg J, Durbeej M: Loss of dystrophin and β-sarcoglycan significantly exacerbates the phenotype of laminin α2 chain-deficient animals. Am J Pathol 2014, 184:740–752
59. Acharyya S, Villalta SA, Bakkar N, Bupha-Intr T, Janssen PM, Carathers M, Li ZW, Beg AA, Ghosh S, Sahenk Z, Weinstein M, Gardner KL, Rafael-Fortney JA, Karin M, Tidball JG, Baldwin AS, Guttridge DC: Interplay of IKK/NF-κB signaling in macrophages and myofibers promotes muscle degeneration in Duchenne muscular dystrophy. J Clin Invest 2007, 117:889–901
60. Bonuccelli G, Sotgia F, Schubert W, Park DS, Frank PG, Woodman SE, Insabato L, Cammer M, Minetti C, Lisanti MP: Proteasome inhibitor (MG-132) treatment of mdx mice rescues the expression and membrane localization of dystrophin and dystrophin-associated proteins. Am J Pathol 2003, 163:1663–1675
61. Assereto S, Stringara S, Sotgia F, Bonuccelli G, Broccolini A, Pedemonte M, Traverso M, Biancheri R, Zara F, Bruno C, Lisanti MP, Minetti C: Pharmacological rescue of the dystrophin-glycoprotein complex in Duchenne and Becker skeletal muscle explants by proteasome inhibitor treatment. Am J Physiol Cell Physiol 2006, 290:C577–C582
62. Bonuccelli G, Sotgia F, Capozza F, Gazzerro E, Minetti C, Lisanti MP: Localized treatment with a novel FDA-approved proteasome inhibitor blocks the degradation of dystrophin and dystrophin-associated proteins in mdx mice. Cell Cycle 2007, 6:1242–1248
63. Selzby J, Morris C, Morris L, Sweeney L: A proteasome inhibitor fails to attenuate dystrophic pathology in mdx mice. PLoS Curr 2012, 4. e4f84a944d8930
64. Azakir BA, Di Fulvio S, Kinter J, Sinnreich M: Proteasomal inhibition restores biological function of mis-sense mutated dysferlin in patient-derived muscle cells. J Biol Chem 2012, 287:10344–10354
65. Mammucari C, Schiaffino S, Sandri M: Downstream of Akt: FoxO3 and mTOR in the regulation of autophagy in skeletal muscle. Autophagy 2008, 4:524–526
66. Langenbach KJ, Rando TA: Inhibition of dystroglycan binding to laminin disrupts the PI3K/AKT pathway and survival signaling in muscle. Muscle Nerve 2002, 26:644–653